Cold Regions Hydrology in a Changing Climate (Proceedings of symposium H02 held during IUGG2011 in Melbourne, Australia, July 2011) (IAHS Publ. 346, 2011).

Distributed modelling of snow- and ice-melt in the Lhasa River basin from 1971 to 2080

MONIKA PRASCH[1], MARKUS WEBER[2] & WOLFRAM MAUSER[1]

1 *Department of Geography, Ludwig-Maximilians-Universität Munich, Luisenstraße 37, 80333 Munich, Germany*
m.prasch@lmu.de

2 *Commission for Glaciology, Bavarian Academy of Sciences, Alfons-Goppel-Straße 11, 80539 Munich, Germany*

Abstract The contribution of melt water release from snow and ice to water availability in mountain regions and adjacent forelands can often only be roughly assessed with simple models, because only sparse data are accessible. The impact of global climate change on water availability thus is afflicted with large uncertainties. We present a distributed modelling approach to determine the contribution of snow- and ice-melt to runoff at a regional scale in the Himalayan basin of the Lhasa River in Tibet under past and future climatic conditions. To fulfil the complex input data requirements, publicly available data are used. The successful validation of the model results for the past proves the application of the approach even in remote regions. Under IPCC SRES A2 climatic conditions with constant precipitation snowmelt will clearly decrease, whereas changes in ice-melt are small, although glacier retreat continues. However, runoff is reduced because of increasing evapotranspiration.

Key words snowmelt; glacier ice-melt; mountain hydrology; climate change; sparse data; Lhasa River, Tibet

INTRODUCTION

Future freshwater availability is a key factor for regional development, as not only drinking water but also food and energy production, health, and industrial development are all, to a certain extent, based on sufficient freshwater supply. In order to mitigate the water-related effects of Global Climate Change (GCC) for societies, appropriate adaptation strategies and Integrated Water Resources Management (IWRM) options for potential changes must be developed. This in turn requires comprehensive knowledge of the future impacts of GCC on the water balance.

Mountainous alpine headwaters play a very significant role in the water balance of many large river basins. The temporal storage of water as snow and ice in the high mountains, and its release during subsequent melting periods to adjacent forelands, makes the water release of snow and glaciers extremely important (Viviroli & Weingartner, 2004). However, the amount of melt water release often can only be roughly assessed with simple models, because sufficient data are seldom accessible in remote mountain regions. The impact of GCC on snow- and ice-melt and accordingly on water availability is thus afflicted with large uncertainties. Particularly in the Himalayas, the timing of the melt-out of glaciers and the adjacent melt water release under future climate conditions is controversial (IPCC, 2007, 2010; Kaltenborn *et al.*, 2010).

To determine the contribution of snow- and ice-melt to runoff in complex, meso- to large-scale watersheds, the spatial heterogeneity of complex basins with mountainous head-watersheds and forelands with large river valleys need to be captured synchronously by models. This includes the simulation of all relevant processes under varying climatic conditions and hydrological regimes. The modelling approach should also be applicable under future climatic conditions. As a consequence, the use of universal parameters, the conservation of mass- and energy, a foundation on physical principles and the abandonment of calibration to measured runoff are required for the modelling approach (Mauser & Bach, 2009). Finally, it should be possible to apply regional climate model (RCM) outputs as future meteorological drivers. Therefore, a complex modelling approach was developed within the framework of the GLOWA-Danube project (www.glowa-danube.de) for the Upper Danube River basin, with an excellent data basis describing the natural and socio-economic characteristics of the watershed. In this paper we present the transferability of the approach to the High Asian basin of the Lhasa River in Tibet with sparse data availability, and solely using publicly available data; the work was carried out within the framework of the Brahmatwinn project (www.brahmatwinn.uni-jena.de).

THE LHASA RIVER BASIN

The Lhasa River basin (LRB) is located in the southern part of the Tibet Autonomous Region of the People's Republic of China in Central Asia (Fig. 1). It is the largest tributary in the middle reach of the Brahmaputra in Tibet, with a basin area of 32 500 km^2. The location on the Tibetan Plateau characterizes the physio-geographic conditions of the watershed. The relief ranges from 3535 m a.s.l. at its junction with the Brahmaputra, up to 7162 m a.s.l. at the peak of the Nyainqêntanglha Mountains, forming the northwestern watershed. Climatic conditions are determined by a strong seasonal course of the precipitation (630 mm), which falls during the monsoon months in summer. Mean annual air temperatures vary between –9°C in the Nyainqêntanglha Mountains to +10°C in the Lhasa River valley near the river's mouth.

Due to the pronounced wet season during the summer monsoon and the dry season lasting the rest of the year, the runoff shows a clear seasonal cycle, with the flood peak reached in August. About 90% of the mean annual runoff is observed between May and November, whereas in the winter season, runoff is low. Most glaciers in the LRB are found along the Nyainqêntanglha Mountains due to their altitude and orientation to the southeast from where the monsoon comes, triggering orographic precipitation. Altogether 670 km^2, equating to 2% of the total basin area, are glacierized (WDC 2009).

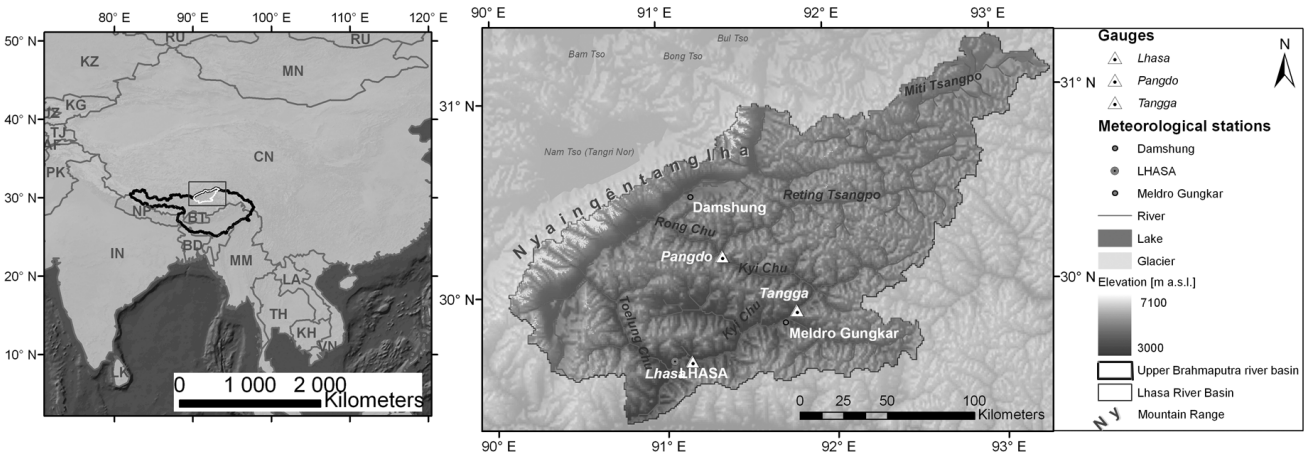

Fig. 1 The Lhasa River basin.

THE MODELLING APPROACH

The models

For the distributed modelling of the hydrological processes in a heterogeneous, large-scale river basin, the PROMET (Processes of Radiation, Mass and Energy Transfer) hydrological model (Mauser & Bach, 2009) was applied. PROMET, which has already been successfully used with changing climatic conditions in the Upper Danube basin (Mauser & Bach, 2009), is a fully spatially distributed raster model with a resolution of 1 × 1 km, and runs on an hourly time step. For simulation of hydrological processes, it uses distinct components for meteorology, land surface energy and mass balances, vegetation, snow and ice, soil hydraulics and soil temperature. Groundwater and channel-flow components with hydraulic structures are also included. As part of the snow and ice component, the SURGES glacier model (Subscale Regional Glacier Extension Simulator) (Weber *et al.*, 2010) was implemented to capture the small-scale processes for simulating ice-melt on alpine glaciers. SURGES uses a subscale parameterization in approximating the heterogeneous glacier surface by subscale units with similar surface elevations. Since the ice-melt water release depends on the snow-free area of the glacier, the duration of the snow cover on all parts of a glacier surface must be calculated. Therefore, the mass and energy balance on the glacier surface, including snow accumulation and ablation, snow metamorphism and glacier

geometry changes are modelled for all elevation levels. The meteorological drivers are provided by the meteorology component of PROMET and extrapolated to all subscale elevation levels.

The components of PROMET fully interact and consider all processes related to water and energy fluxes. Within, as well as throughout all its components and feedbacks, PROMET strictly conserves mass and energy. The model characteristics allow the simulation of all relevant processes under varying climatic conditions and hydrological regimes. Furthermore, PROMET is not calibrated in using measured discharge data to fully exploit the predictive capabilities of the physically-based approach. It can therefore be used under past as well as future climatic conditions (Mauser & Bach, 2009). Additionally, these characteristics form the basis for coupling with RCMs, which are also usually raster-based. Since the spatial resolution of RCM outputs is in the range of 100 to 1000 km^2, the gap between this scale and the resolution of 1 km^2 of PROMET must be closed. Therefore the SCALMET (Scaling Meteorological variables) (Marke, 2008) coupling tool refines the coarse resolution of the RCM outputs in using different scaling techniques. They range from direct interpolation methods, such as bilinear interpolation, to statistical approaches using empirical relations. A combination of physically-based and statistical methods is also applied. Not only air temperature and precipitation are downscaled with these methods, but also wind speed, longwave and shortwave radiation, humidity and surface pressure, which are especially important for the simulation of snow and ice processes.

Derivation of input data

For the detailed simulation of the water flow considering snow and ice-melt water, vegetation growth, soil texture, groundwater flow and finally the interaction in routing the water in the river channel by the PROMET components, air temperature, precipitation, air humidity, wind speed and incoming short- and longwave radiation are required as meteorological drivers for past and future climate conditions. RCM outputs of the COSMO-CLM ERA 40 and ECHAM 5 model runs are used in this study as input data for SCALMET. Within the framework of the Brahmatwinn project, bias correction methods were applied to the CLM air temperature as well as to precipitation during the monsoon months in the whole Upper Brahmaputra basin, as described in Dobler & Ahrens (2008).

Additionally, data describing topography, land use and land cover, soil texture, river bed characteristics and glacier geometry are required to run the models. Gridded GIS layers describe the spatial distribution of the required parameters in the basin, whereas plant and soil parameters are provided in data tables for each land cover and soil texture class, because they are assumed to be homogenous throughout the whole catchment. Since sparse data is available for the LRB, publicly accessible data is used.

For topographic properties, the digital elevation model of the Shuttle Radar Topography Mission SRTM (Jarvis *et al.*, 2006) was applied in the LRB. Slope and aspect were deduced from the digital elevation model using the terrain analysis tool TOPAZ (Gabrecht & Martz, 1999), which was also applied to derive the watershed of the catchment, the main channel network with the channel slope and the flow direction. They, in turn, are required to run the river routing component of PROMET. Channel width is also needed. It was derived under the assumption that it correlates with the accumulated upstream area, also provided by TOPAZ, consistent with Mauser & Bach (2009). To determine the flow velocity, Manning's roughness parameter, which was deduced by field data, was applied. For the simulation of groundwater flows, the distance to the main river channel is required, which is also provided by TOPAZ. Depending on the distance, the storage time constant is set between one hour and one year.

The NASA TERRA/MODIS land cover product (Boston University, 2004) provides information about land cover and land use in the LRB. The parameterization of the land-use classes was adopted from Europe and adapted to the conditions of Tibet according to literature and field data. In order to model the water processes in the soil, soil texture classes were taken from the Harmonized World Soil Database (FAO *et al.*, 2009). The required parameters for the classes were adapted from the parameterization according to Mauser & Bach (2009).

In order to run SURGES, the area–elevation distribution of all glaciers and the ice thickness for all elevation levels is required as input data for all glacierized grid cells in the test basin. In general, the availability of glacier data is poor in the LRB, but the Chinese Glacier Inventory (CGI) provides polygons of the glacier areas of 1970 and additional information of their mean ice thickness (WDC, 2009). By intersecting the glacier boundaries with the ASTER Global Digital elevation model GDEM (ERSDAC, 2009) and aggregating the elevation values to levels at intervals of 100 m, the elevation levels for all glaciers in the LRB are deduced. Within the aggregation steps, the slope is averaged by weighting of the area. In this process, each glacier is considered separately, and so the elevation levels are not aggregated among different glaciers. Next, the area per elevation level is calculated. To consider the different ice thickness distribution of a glacier in more detail than assuming a homogenous ice block, the mean ice thickness provided by the CGI is modified for all elevation levels of the glacier. Thereby a correlation between surface slope and ice thickness (Haeberli & Hoelzle, 1995), and the thinning out of the glacier to its edges and the glacier front are considered.

Validation

While the uncertainty of the glacier area is in the 5% range (Wang *et al.*, 2009), the accuracy of the GDEM varies between ±7–14 m (ERSDAC, 2009). Because the elevation model was recorded in the year 2000 and is combined with the glacier boundaries of 1970, on average about 6–10 m w.e. (water equivalent) (Frauenfelder & Kääb, 2009) has melted away. Consequently, the elevation data are slightly too low. However, this average value is approximately within the range of accuracy of the elevation model. To check the quality of the deduced ice thickness for the elevation levels as described above, the derivation method was applied in the Eastern Alps, where area and geometry of the glaciers are similar to glaciers in the LRB, because no data are available in the LRB. The deduced ice volumes were compared to the data of the Austrian Glacier Inventory (Lambrecht & Kuhn, 2007). The volume deduced is 2% smaller, which corresponds to a deviation of 1 m ice thickness. Finally, the volumes of the elevation levels of a mountain and a valley glacier were compared. The overall deviation varies between 3 and 6%, which corresponds to a difference of 2 m or 3 m, respectively, of mean ice thickness. In comparison to uncertainties of ice thickness values for the Austrian Alps of between 5 and 10% (Fischer, 2009), the deviation is small. Additionally, the deviations are also within the accuracy range of the digital elevation model.

Detailed validation studies of the PROMET model components, including SURGES and SCALMET, have proven the quality of the model (Marke, 2008; Mauser & Bach, 2009). Its performance in the LRB is thus shown here. First, the downscaled ECHAM 5-driven CLM data are compared to average recordings of the three meteorological stations Lhasa, Damshung and Meldro Gungkar (see Fig. 1) from 1980 to 2000 in the LRB. While air temperature is reproduced, the deviations of the precipitation sum are between 10 and 22%. Next, glacier changes are validated. Glacier mass balances of –0.2 to –0.3 m w.e. per year between 1970 and 2000 and an area retreat of 21% in the LRB (Frauenfelder & Kääb, 2009) are in accordance to the simulated –0.3 m w.e. per year and an area loss of 20%. Finally, the mean simulated runoff is compared to three station observations of Lhasa, Pangdo and Tangga between 1996 and 2000. The deviation is below 5%. Since the ECHAM 5-driven CLM data can only reproduce the climate signal, ERA 40-driven CLM data are applied for the validation of monthly runoff data at the three gauges. Figure 2 shows the correlation between modelled and observed runoff with coefficients of determination of 0.87 to 0.89 and Nash-Sutcliffe efficiency coefficients (Nash & Sutcliffe, 1970) between 0.84 and 0.88.

The validation results prove the reproduction of glacier and hydrological dynamics in the LRB during past climatic conditions by the modelling approach. In order to determine the impact of future climate change on the melt water release of snow and ice and accordingly on runoff, results of the CLM ECHAM-5 driven model runs under IPCC SRES scenario A2 conditions are presented until 2080.

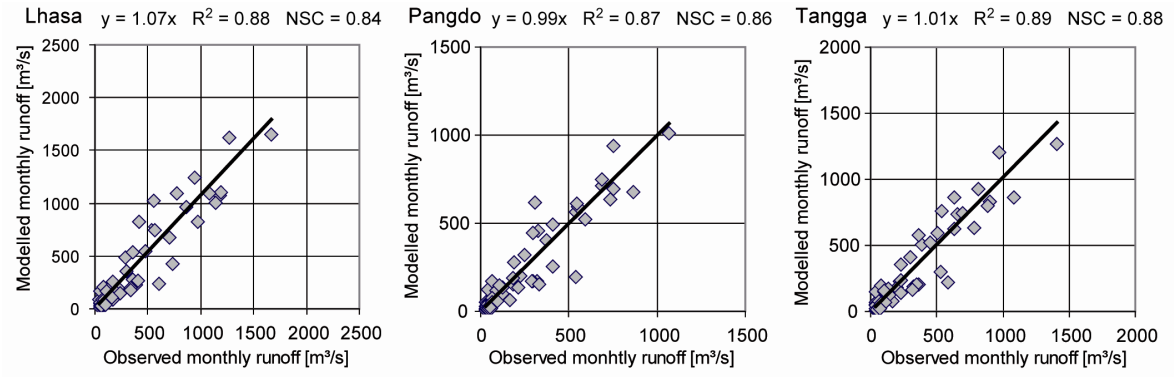

Fig. 2 Comparison of monthly modelled and observed runoff at the Lhasa, Pangdo and Tangga gauges from 1996 to 2000.

RESULTS

The mean annual air temperature in the LRB of –0.1°C between 1971 and 2000 will increase by 4.3 K until 2080 according to the A2 scenario. Although no significant trend is simulated for the amount of precipitation of 630 mm in the LRB, the percentage of snowfall is clearly reduced from 28% (1971–2000) to 15% . The spatial comparison of the percentage of snowfall between the past and the future periods from 2011–2040 and 2051–2080 is shown in Fig. 3(a). The highest proportion of snowfall is reached along the Nyainqêntanglha Mountains and in the northeastern parts of the basin, with 40–100%. From 2011 to 2040, the reduction rises to 10% for almost the entire basin area, and reaches 20% in the northeastern Nyainqêntanglha Mountains. The spatial pattern of the trend continues in the 2051–2080 period in accordance with the increasing air temperature. A maximum reduction of 30% is reached in the high mountain regions. This means a reduction of up to 3 months in the snow cover duration throughout the LRB.

The considerable changes in the meteorological conditions result in a proceeding glacier retreat under A2 scenario conditions in the LRB. The spatial distribution of the ice water reservoir is shown for 1970, 2000, 2040 and 2080 in Fig. 3(b). The changes in the past period are small, but glaciers did melt, particularly at their edges. In the scenario simulations, the retreat until 2040 is again small, but some glaciers in the northeastern parts disappear. Afterwards, an accelerating melt is simulated, and large storages with reservoirs greater than 50 m w.e. per km^2 decrease. More grid cells lose glacierization. Only around the Nyainqêntanglha Mountain peak is an amount larger than 50 m w.e. per km^2 stored as glacier ice in 2080, whereas a level of 25 m w.e. is rarely exceeded in all the other regions. The glaciers in the northeast melt completely.

The simulated changes in snow and ice reservoirs impact the amount of snow- and ice-melt released. The amount of snowmelt has, in accordance with snow precipitation, been decreasing since 1970. This negative trend continues until the end of the simulation period in 2080. As a result, the 215 mm mean amount of the past is reduced by 101% in the A2 model until 2080 (Fig. 4). In contrast to the uniformly negative trend of the amount of snowmelt, the future development of ice-melt water release varies in the scenario. The development of ice-melt shows a slight decrease from 12 to 8 mm until 2040. Afterwards, the amount increases and exceeds 15 mm. The total amount of ice-melt water is small, however, and accounts only for one fifth of the snowmelt (Fig. 4). The clear decrease of glacial coverage and stored ice water equivalent is therefore not pronounced in the course of the ice-melt. Shorter snow periods, because of higher air temperatures, enable the melting of ice at higher elevations. As a consequence, the reduction of the ice water reservoir is balanced by larger or longer snow-free glacier areas.

In assessing future water availability, important water balance values include not only precipitation, snow- and ice-melt amounts, but also the development of evapotranspiration. In accordance with the rising air temperature, evapotranspiration increased slightly during the period 1971–2000. This positive trend continues in the future A2 simulations and reaches an increase of 22% by 2080.

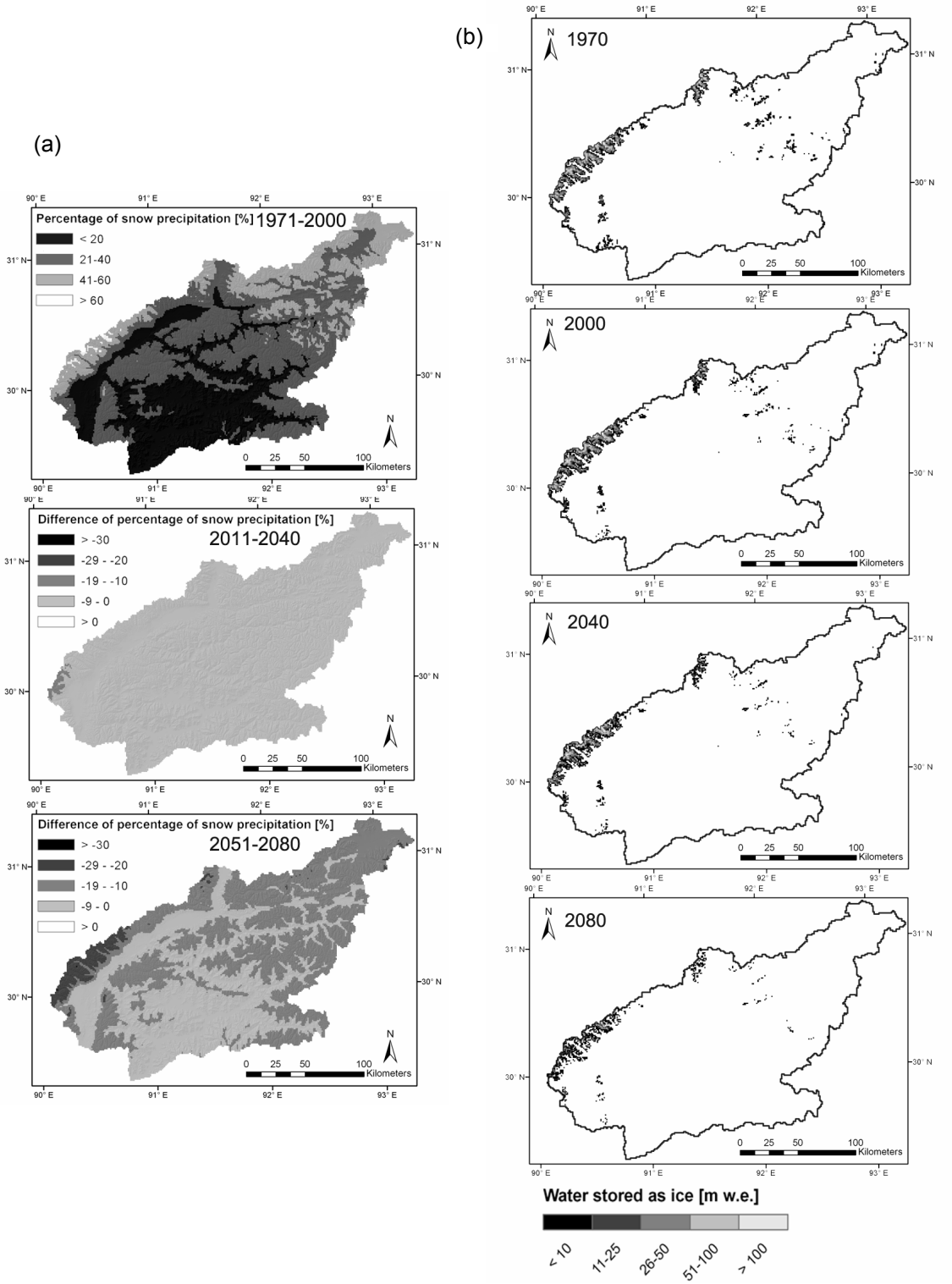

Fig. 3 (a) Percentage of snowfall. (b) The simulated ice water equivalent distribution in 1970, 2000, 2040 and 2080.

All the factors described above, together with soil water content and groundwater changes, determine the river runoff. Figure 4 shows the course of the mean annual discharge at the catchment outlet of the Lhasa River, together with precipitation, evapotranspiration and snow- and ice-melt. Since no trend is simulated for soil water content and groundwater changes, they are not

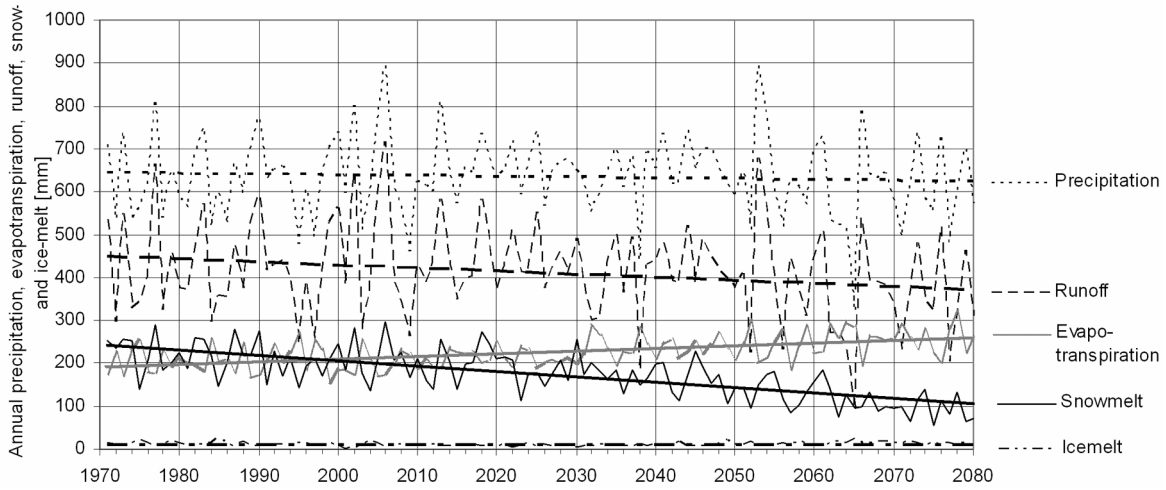

Fig. 4 Development of annual water balance parameters in the LRB from 1971 to 2080.

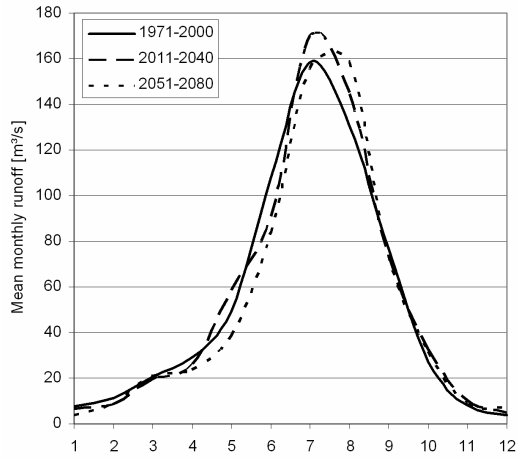

Fig. 5 Development of mean monthly runoff at the LRB outlet gauge for three climate periods.

illustrated. Runoff significantly decreases under A2 scenario conditions. While the amount of precipitation almost stays constant, the changes in runoff can be traced back to the increasing evapotranspiration.

Although the amount of ice-melt increases after 2050, as analysed above, the total amount is too small in comparison to other water balance components to influence runoff at the outlet gauge of the LRB. Thus, the mean annual runoff is determined by precipitation and follows its amount.

Snowmelt is of minor influence for the annual values, but it is relevant for the seasonal course of runoff. Accordingly, the comparison of mean monthly runoff for three climate periods (Fig. 5) shows a decrease from April to June, which is significant in May and June due to the trend analysis based on Mann (1945) and Kendall (1970). Since less precipitation is stored as snow than in the past period, less water is released as runoff in spring. The decrease of 18 to 22% (2051–2080 to 1971–2000) in these months is within the model accuracy with coefficients of determination of 0.87 to 0.89 and biases between 1 and 7% (see Fig. 2).

CONCLUSION

The presented approach enables the analysis of the future impact of GCC on water availability in the LRB and thus provides a basis for developing IWRM adaptation strategies. Although the

models require a broad range of input data due to the complexity of the subject to be modelled, this study demonstrates their applicability in remote regions by using publicly available data. The analysis of the model results shows the dominant dependency of the Lhasa River runoff on precipitation and evapotranspiration. The amount of snowfall and the subsequent duration of snow cover determine the seasonal course, which follows the monsoon precipitation, peaking in summer. Under average climatic conditions, the amount of melt-water contribution from glacier ice, considered independently of snowmelt release, is too small to influence runoff at the catchment outlet, although glacier retreat continues according to the IPCC SRES A2 scenario run. Accordingly, runoff decrease is mainly caused by increasing evapotranspiration in the LRB in this scenario.

Acknowledgements Financial support by the European Commission Sixth Framework Programme (FP6) within the project "Brahmatwinn" and the Federal Ministry of Education and Research (BMBF) within the "GLOWA-Danube" project are gratefully acknowledged. We thank the Institute of Tibetan Plateau Research ITP and the International Centre for Integrated Mountain Development ICIMOD for data provision.

REFERENCES

Boston University (2004) NASA TERRA/MODIS HDF-EOS MOD12Q1 V004 Land Cover Product Binary Data, Eurasia subset, IGBP Class Scheme, available from http://duckwater.bu.edu/lc/mod12q1.html.

Dobler, A. & Ahrens, B. (2008) Precipitation by a regional climate model and bias correction in Europe and South Asia. *Met. Z.* **17**(4), 499–509.

ERSDAC (Earth Remote Sensing Data Analysis Center) (2009) The Ministry of Economy, Trade, and Industry (METI) of Japan and the United States National Aeronautics and Space Administration (NASA): Aster Global Digital Elevation Model (GDEM), available from http://www.ersdac.or.jp/GDEM/E/2.html.

FAO, IIASA, ISRIC, ISSCAS & JRC (2009) *Harmonized World Soil Database* (version 1.1). FAO, Rome, Italy and IIASA, Laxenburg, Austria.

Fischer, A. (2009) Calculation of glacier volume from sparse ice-thickness data, applied to Schaufelferner, Austria. *J. Glaciol.* **55**(191), 453–460.

Frauenfelder, R. & Kääb, A. (2009) Glacier mapping from multi-temporal optical remote sensing data within the Brahmatwinn river basin. *Proc. of the 33rd International Symposium on Remote Sensing of Environment* (May 2009, Stresa, Italy).

Garbrecht, J. & Martz, L. W. (1999) *TOPAZ Version 3.1*. USDA, Agricultura Research Service Grazinglands Research Laboratory, Oklahoma, USA.

Haeberli, W. & Hoelzle, M. (1995) Application of inventory data for estimating characteristics of and regional climate-change effects on mountain glaciers: a pilot study with the European Alps. *Annals of Glaciology* **21**, 206–212.

IPCC (2007) Asia. In: *Climate Change 2007: Impacts, Adaptation and Vulnerability.* Contribution of Working Group II to the Fourth Assessment Report of the Intergovernmental Panel on Climate Change (ed. by M. L. Parry, O. F. Canziani, J. P. Palutikof, P. J. Van Der Linden & C. E. Hanson), Cambridge University Press, Cambridge, UK.

IPCC (2010) IPCC statement on the melting of Himalayan glaciers. Geneva, 20 January 2010, Switzerland. Available from: http://ipcc-wg2.gov/publications/AR4/himalayastatement-20january2010.pdf

Jarvis, A., Reuter, H. I., Nelson, A. & Guevara, E. (2006) Hole-filled seamless SRTM data V3, International Centre for Tropical Agriculture (CIAT), available from http://srtm.csi.cgiar.org.

Kaltenborn, B. P., Nellemann, C. & Vistnes, I. I. (eds) (2010) *High Mountain Glaciers and Climate Change. Challenges to Human Livelihoods and Adaptation*, UN Environment Programme, GRID-Arendal, Birkeland Trykkeri AS, Norway.

Kendall, M. G. (1970) *Rank Correlation Methods* (4th edn). Griffin, London, UK.

Lambrecht, A. & Kuhn, M. (2007) Glacier changes in the Austrian Alps during the last three decades, derived from the new Austrian glacier inventory. *Annals of Glaciology* **46**, 177–184.

Mann, H. B. (1945) Nonparametric test against trends. *Econometrica* **13**, 245–259.

Marke, T. (2008) Development and application of a model interface to couple regional climate models with land surface models for climate change risk assessment in the Upper Danube Watershed. PhD Thesis, LMU München, Germany, available from http://edoc.ub.uni-muenchen.de/9162/ .

Mauser, W. & Bach, H. (2009) PROMET – Large scale distributed hydrological modelling to study the impact of climate change on the water flows of mountain wastersheds. *J. Hydrol.* **376**, 362–377.

Nash, J. E. & Sutcliffe, J. V. (1970) River flow forecasting through conceptual models. Part I – A discussion of principles. *J. Hydrol*. **10**(3), 282–290.

Viviroli, D. & Weingartner, R. (2004) The hydrological significance of mountains: from regional to global scale. *Hydrol. Earth System Sci.* **8** (6), 1016–1029.

Wang., Y., Hou, S.& Liu, Y. (2009) Glacier changes in the Karlik Shan, eastern Tien Shan, during 1971/72 – 2001/02. *Annals of Glaciology* **50**(53), 39–45.

WDC (2009) Chinese Glacier Inventory of the World. Data Center For Glaciology and Geocryology, Lanzhou, China. Available from http://wdcdgg.westgis.ac.cn/DATABASE/Glacier/glacier_inventory.asp.

Weber, M., Braun, L., Mauser, W. & Prasch, M. (2010) Contribution of rain, snow- and icemelt in the Upper Danube discharge today and in the future. *Geogr. Fis. Dinam. Quat*. **33**(2), 221–230.